Kelvin-Helmholz instability in heavy ions

2nd International Symposium on Non-equilibrium Dynamics

and 3rd TURIC Network Workshop,

25 - 30 June 2012, Hersonissos,

Crete, Greece,

L.P. Csernai

Outline

- Initial state / peripheral collision
- Increasing angular momentum
- Rotation
- Small viscosity (→ fluctuations & instabilities)
- Kelvin-Helmholtz Instability (KHI)
- Sensitive to viscosity and shear flow

How to conserve momentum?

At low energies – fire streak picture

[Myers, Gosset, Kapusta, Westfall]

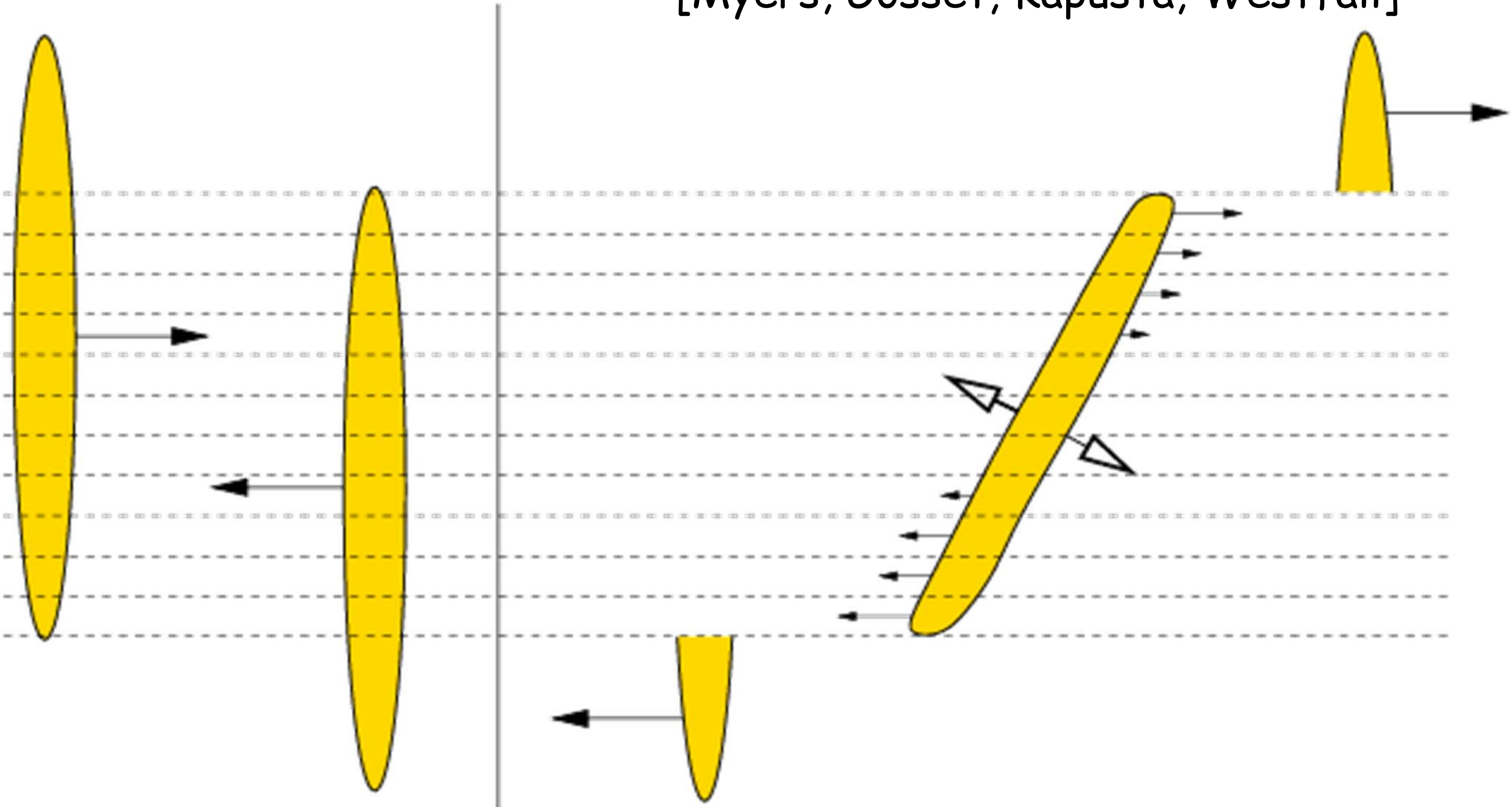

Tilted initial state

Before collision

The "firestreak" initial state

Initial state – reaching equilibrium

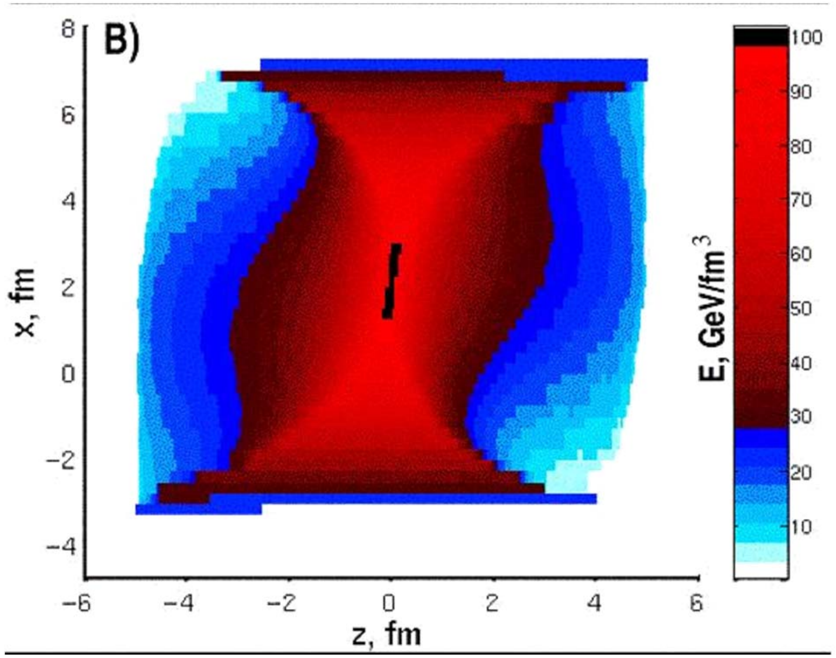

Initial state by V. Magas, L.P. Csernai and D. Strottman

Phys. Rev. C64 (2001) 014901

Nucl. Phys. A 712 (2002) 167–204

M1

PIC method:

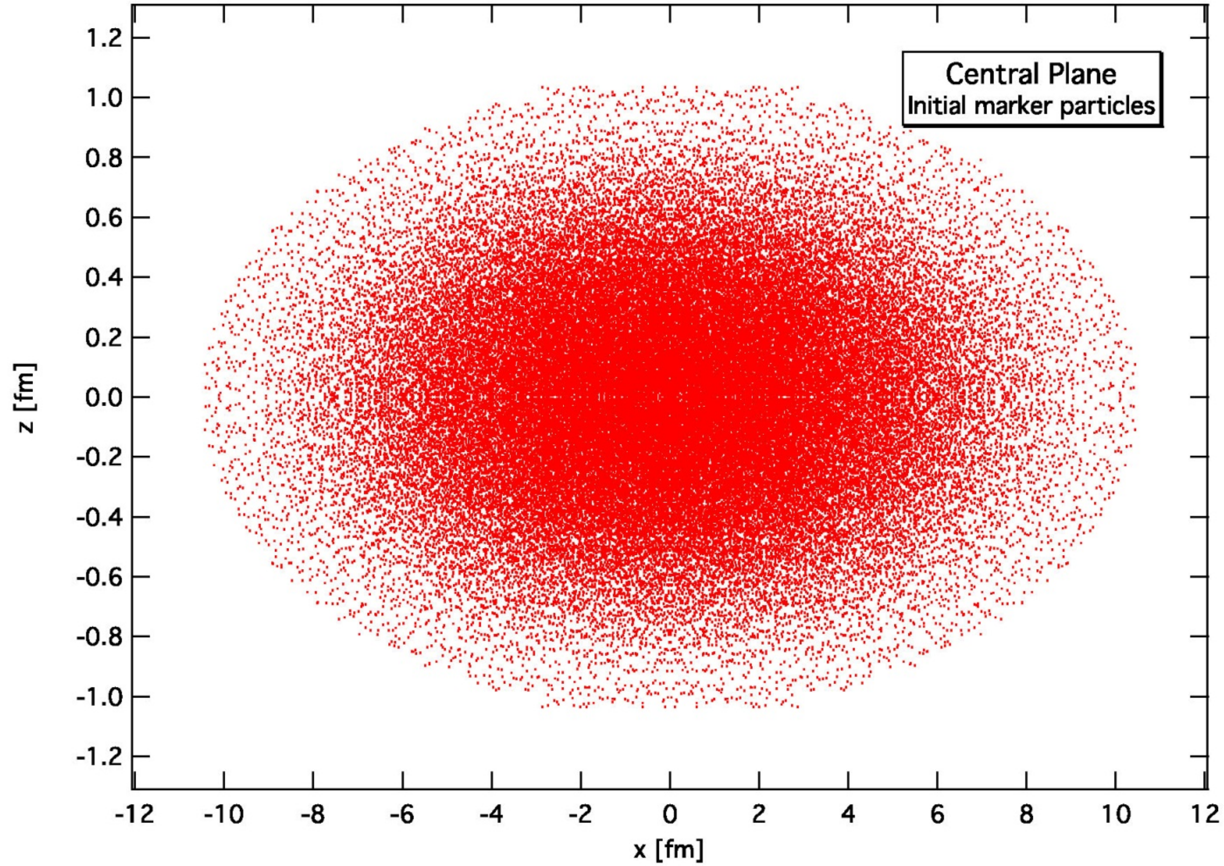

Figure: In the PIC method Lagrangian fluid elements, called Markers, move in a decartian coordinate grid. At very high energies, to avoid instabilities arising from the computational grid, marker particles are randomized in our approach. The figure shows Marker particle positions in the central plane of an explosion (z is the beam direction), assuming an initial Landau state [15] with an energy density of 40 GeV/fm3. A total of 1.5 million marker particles are used to describe the three-dimensional nucleus [unpublished].

M2

PHYSICAL REVIEW C **84**, 024914 (2011)

Fluid dynamical prediction of changed v_1 flow at energies available at the CERN Large Hadron Collider

L. P. Csernai,[1,2,3] V. K. Magas,[4] H. Stöcker,[3] and D. D. Strottman[1,3]

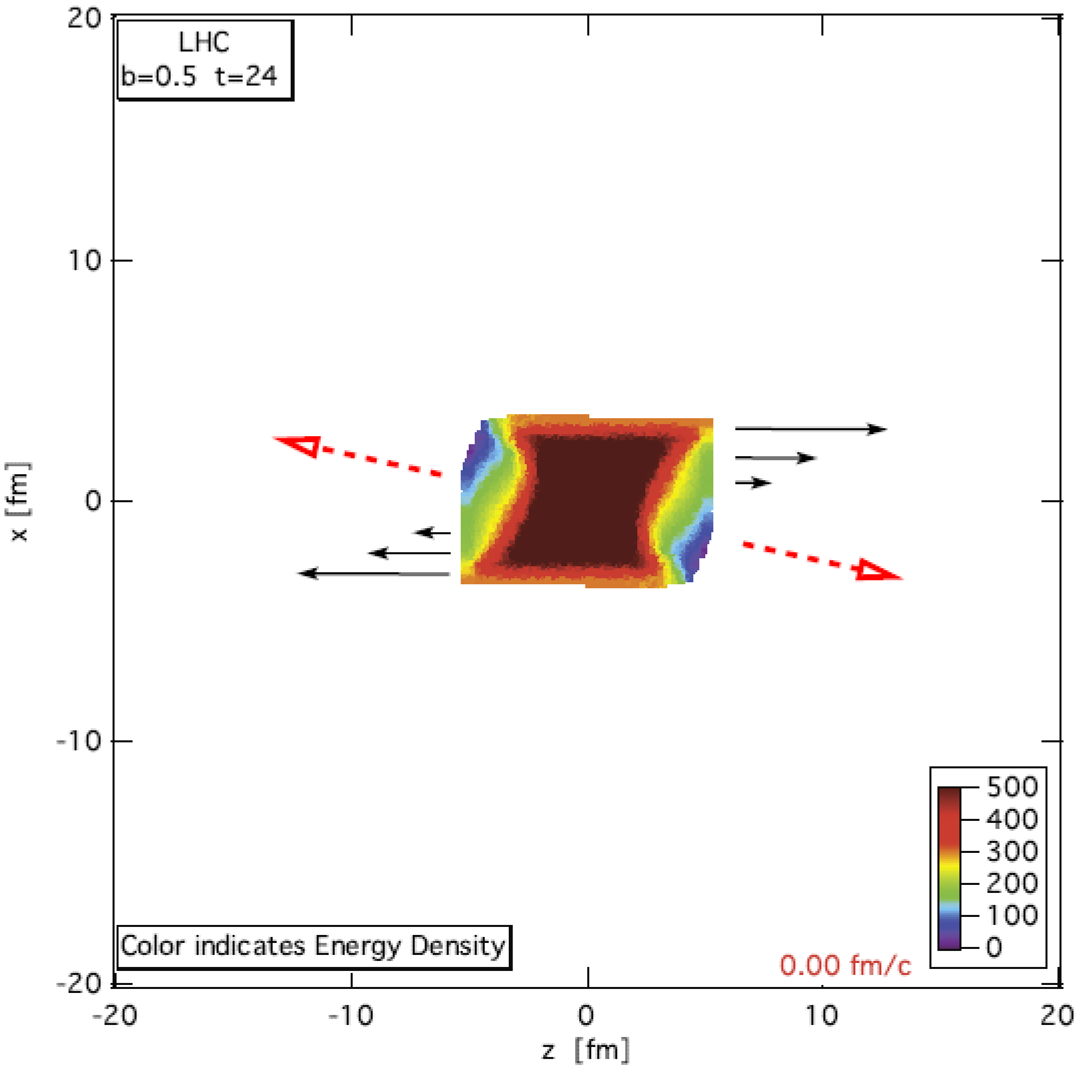

Anti-flow (v1) at LHC

Initial energy density [GeV/fm3] distribution in the reaction plane, [x,y] for a Pb+Pb reaction at 1.38 + 1.38 ATeV collision energy and impact parameter b = 0.5_bmax at time 4 fm/c after the first touch of the colliding nuclei, this is when the hydro stage begins. The calculations are performed according to the effective string rope model. This tilted initial state has a flow velocity distribution, qualitatively shown by the arrows. The dashed arrows indicate the direction of the largest pressure gradient at this given moment.

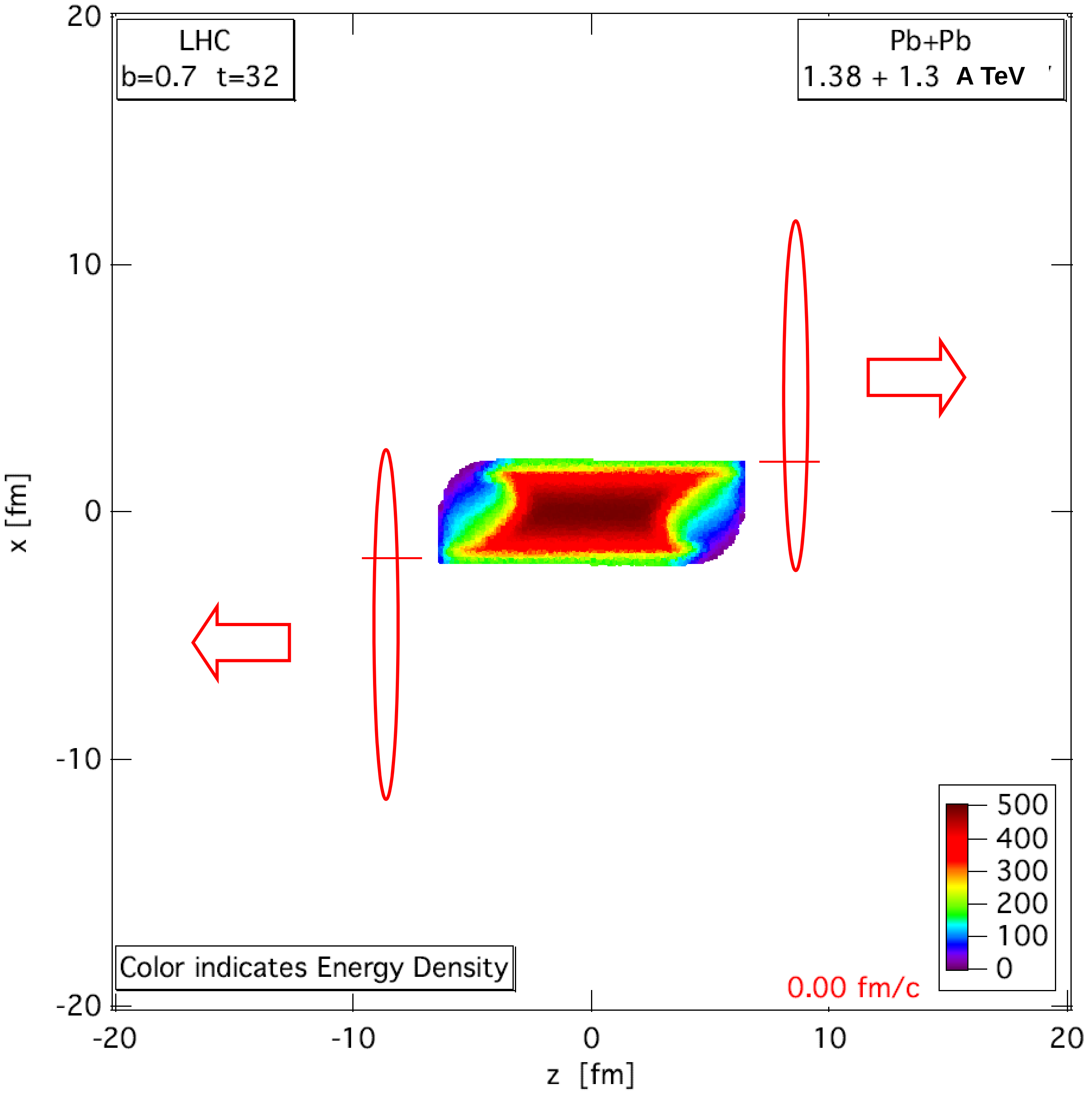

PIC-hydro

Pb+Pb 1.38+1.38 A TeV, b= 70 % of b_max

Lagrangian fluid cells, moving, ~ 5 mill.

MIT Bag m. EoS

FO at T ~ 200 MeV, but calculated much longer, until pressure is zero for 90% of the cells.

Structure and asymmetries of init. state are maintained in nearly perfect expansion.

..\zz-Movies\LHC-Ec-1h-b7-A.mov

Anti-flow (v1)

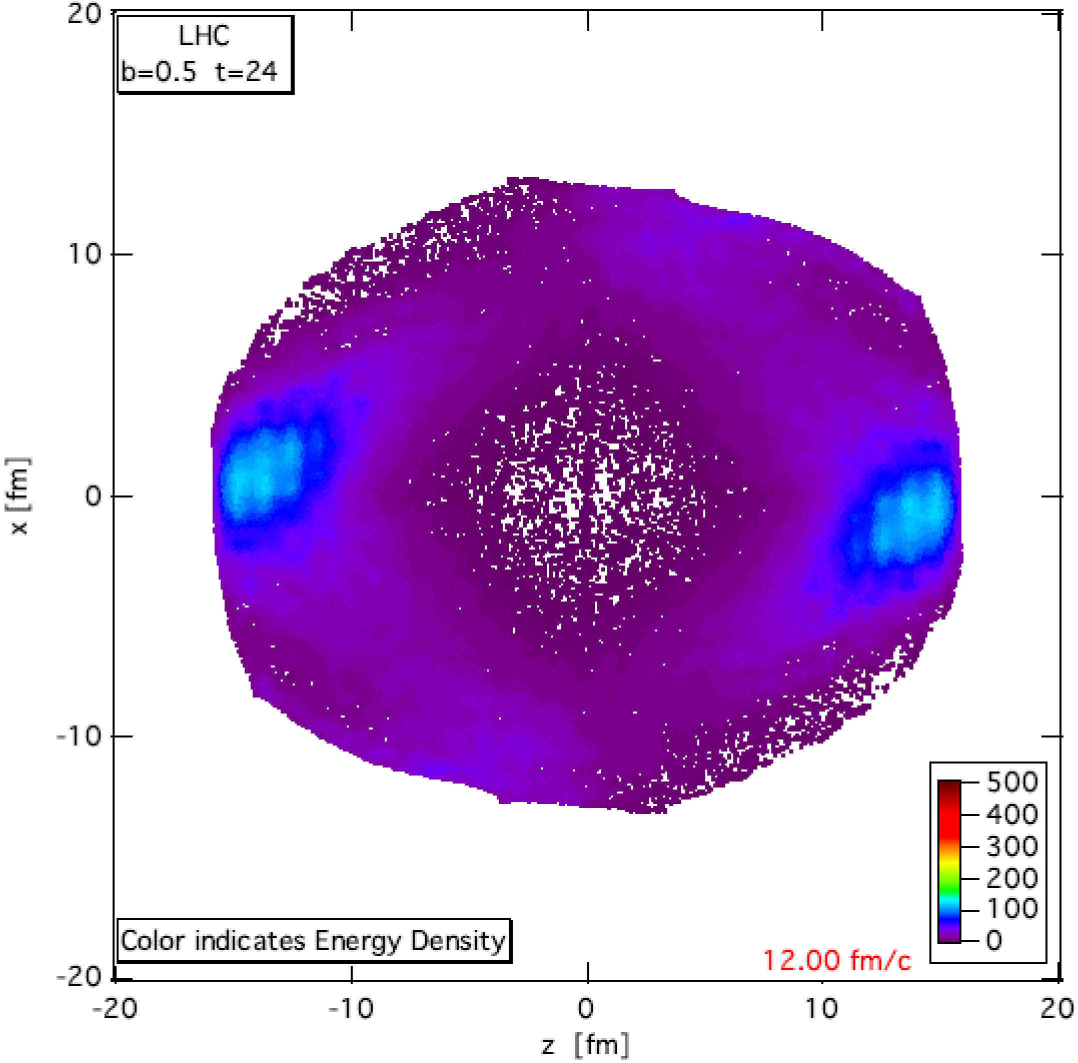

The energy density [GeV/fm3] distribution in the reaction plane, [x,z] for a Pb+Pb reaction at 1.38 + 1.38 A.TeV collision energy and impact parameter b = 0.5b_max at time 12 fm/c after the formation of the hydro initial state. The expected physical FO point is earlier but this post FO configuration illustrates the flow pattern.

[LP. Csernai, VK. Magas, H. Stocker, D. Strottman, arXiv: 1101.3451 (nucl-th)]

Anti-flow (v1)

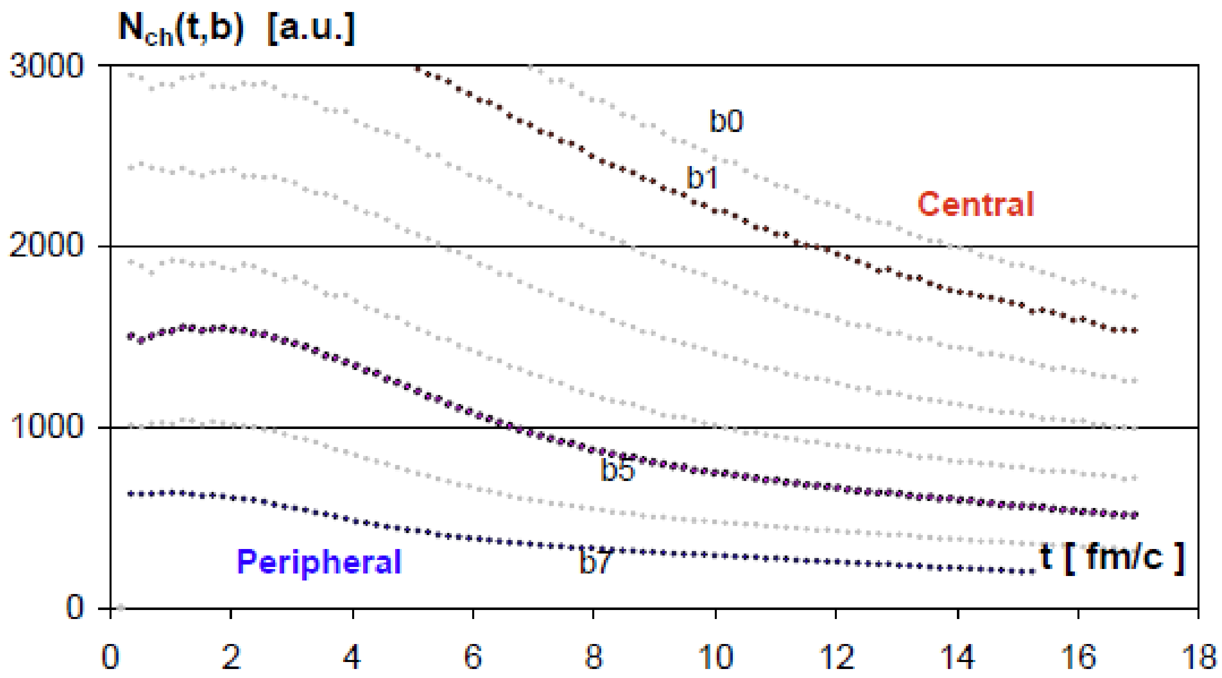

The calculated charged particle multiplicity, N_ch, as a function of FO time (assuming a t_FO = const: FO hyper-surface), for different impact parameters, b = 0.0; 0.1; 0.2; … 0.7 b_max. The indicated (b0, b1, ... b7) FO times for different impact parameters reproduce the measured charged particle multiplicities, N_ch, in the corresponding centrality bins. The visible fluctuations arise from the feature of the PIC method, that the volume increases by one cell when a marker particle crosses the boundary. Thus at the initial state with relatively few cells and large relative surface, this leads to fluctuations.

Anti-flow (v1)

Using the Cooper-Frye FO formula, we can obtain the v_n(pt) and v_n(y) flow components, for massless pions:

$$v_n(y) = \frac{\sum_i^{cells} J_n(y, \vec{v}^{\,i}, T^i) cos(n\phi_0^i)}{\sum_i^{cells} J_0(y, \vec{v}^{\,i}, T^i)}\,, \qquad (2)$$

$$J_n(y, \vec{v}^{\,i}, T^i) = \int_0^\infty dp_t p_t^2 I_n(\gamma_t^i v_t^i p_t / T^i) e^{-\gamma_t^i p_t cosh(y - y_0^i)/T^i}\,,$$

Conservation laws are satisfied at a constant time FO hyper-surface.

$$v_n(p_t) = \frac{\sum_i^{cells} B(\vec{v}^{\,i}, T^i, p_t) I_n(\gamma^i v_t^i p_t / T^i) cos(n\phi_0^i)}{\sum_i^{cells} B(\vec{v}^{\,i}, T^i, p_t) I_0(\gamma^i v_t^i p_t / T^i)}\,, \qquad (3)$$

$$B(\vec{v}, T, p_t) = e^{-\gamma p_t / T} \frac{1}{1 - v_z^2} \left(v_z \frac{T}{\gamma} - p_t |v_z| \right)$$

$$+ \frac{p_t}{\sqrt{1 - v_z^2}} K_1 \left(\frac{\gamma p_t \sqrt{1 - v_z^2}}{T}, \frac{\gamma p_t}{T} \right)\,.$$

L.P. Csernai

Anti-flow (v1)

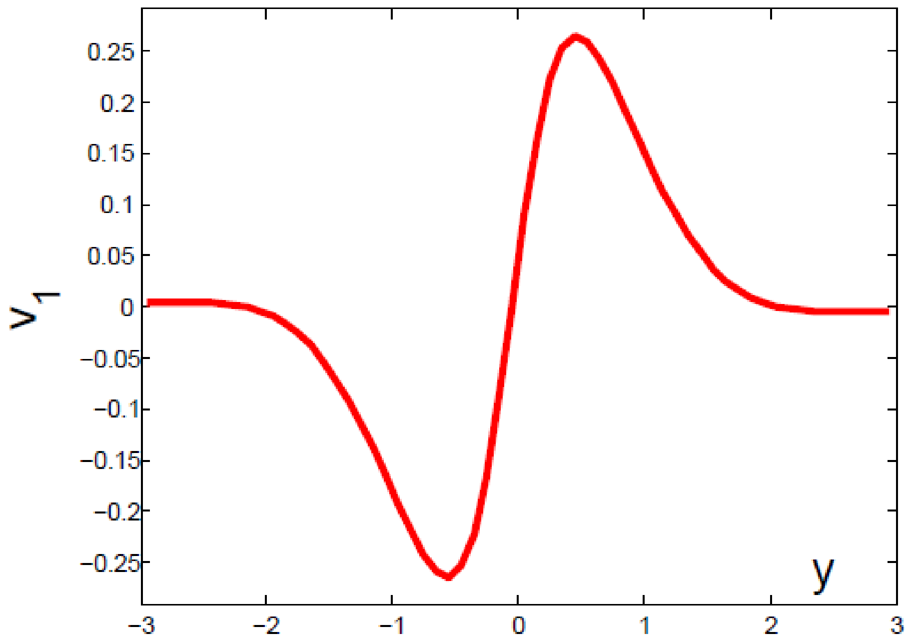

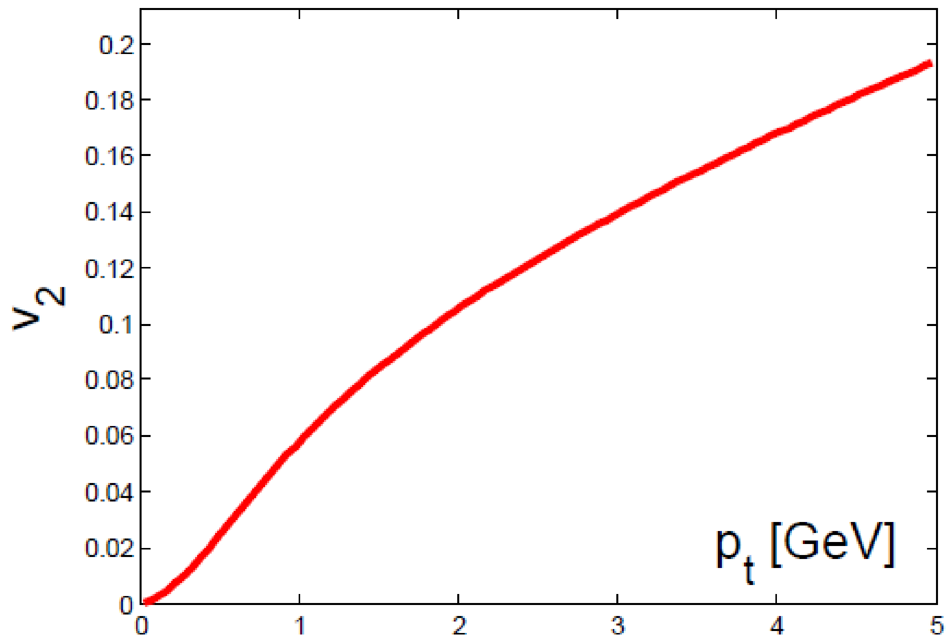

The v_1 & v_2 parameter calculated for ideal massless pion Juttner gas, versus the transverse momentum, p_t, for b = 0.7b_max, at t = 8 fm/c FO time. The magnitude of v_2 is comparable to the observed v_2 at 40-50 % centrality. The v_2 value is slightly below the experimental data, which can be attributed to integral over the whole rapidity range, while the experiment is only for η < 0.8. The v1 peak appears at positive rapidity, in contrast to lower energy calculations and measurements.

Anti-flow (v1)

Initial state CM rapidity fluctuations were taken into account

$$N_{part} m_N \sinh(\triangle y_{CM}) = m_N \sinh(y_0) \Rightarrow$$
$$\triangle y_{CM} = \sinh^{-1}\left[\sinh(y_0)/N_{part}\right] = 3.8\,.$$

Vs_1 (pt) is not sensitive to the initial state y_CM fluctuations

$$v_1^S(p_t) = \frac{\sum_i^{cells} 2D(\vec{v}^{\,i}, T^i, p_t) I_1(\gamma^i v_t^i p_t / T^i) cos(\phi_0^i)}{\sum_i^{cells} B(\vec{v}^{\,i}, T^i, p_t) I_0(\gamma^i v_t^i p_t / T^i)}, \tag{4}$$

Elliptic-flow (v2)

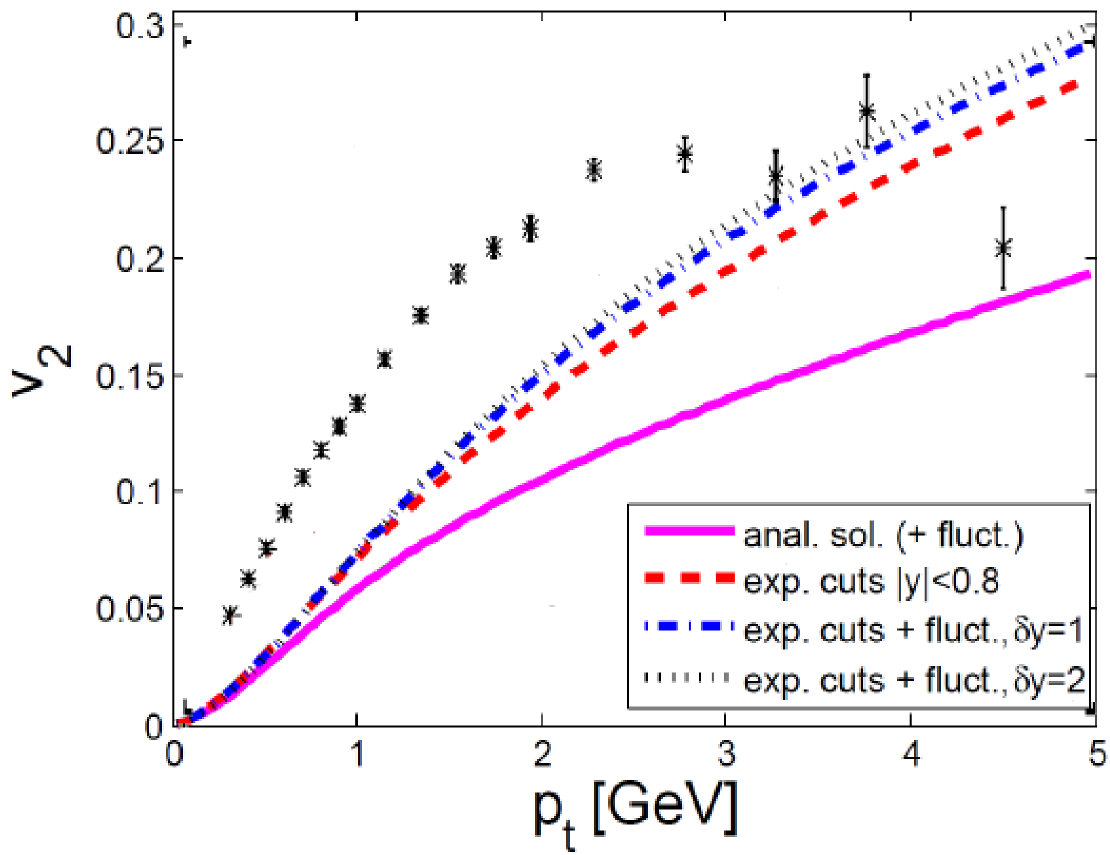

The v_2 parameter calculated for ideal massless pion Juttner gas, versus the transverse momentum, p_t for b = 0.7 b_max, at t = 8 fm/c FO time. The magnitude of v_2 is comparable to the observed v_2 at 40-50 % centrality (black stars).

Anti-flow (v1)

Initial fluctuations in the positions of nucleons in the transverse plane

→different number of participants from projectil and target

→Reduce v_1 at central rapidities, as v1 has a sharp change at y=0, and the initial fluctuations have not.

→v_1 is reduced but still measurable

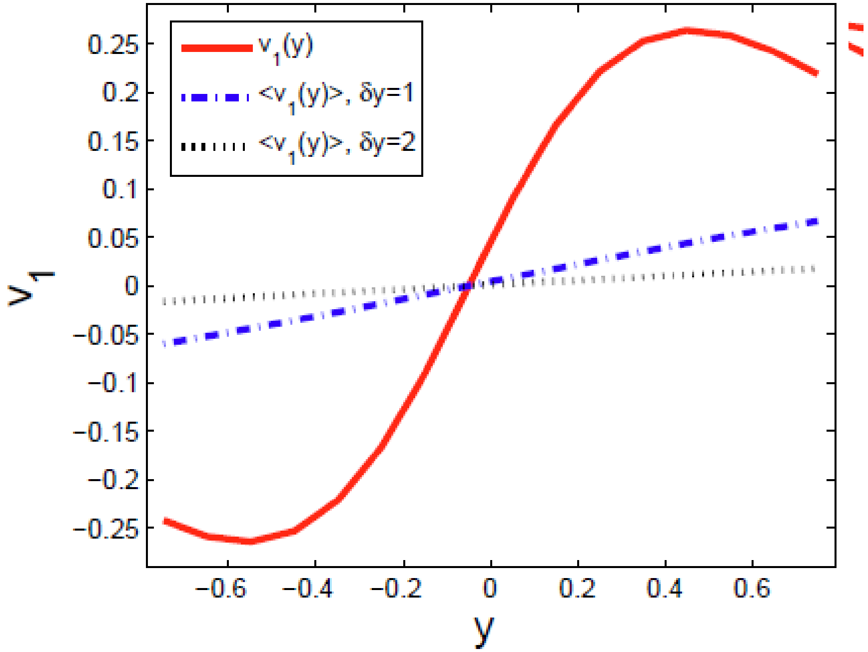

[Yun Cheng, et al., Phys. Rev. C ***84*** *(2011)* 034911.]

Method to compensate for C.M. rapidity fluctuations

1. Determining experimentally EbE the C.M. rapidity
2. Shifting each event to its own C.M. and evaluate flow-harmonics there

L.P. Csernai[1,2], G. Eyyubova[3] and V.K. Magas[4]

arXiv:1204.5885v1 [hep-ph]

Determining the C.M. rapidity

The rapidity acceptance of a central TPC is usually constrained (e.g for ALICE $|\eta| < \eta_{lim} = 0.8$, and so: $|\eta_{C.M.}| << \eta_{lim}$, so it is not adequate for determining the C.M. rapidity of participants.

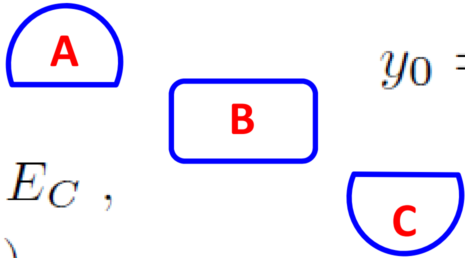

$$y_0 = 7.986$$

Participant rapidity from spectators

$$E_B = A_B\ m_{B\perp}\ \cosh(y^B) = E_{tot} - E_A - E_C\ ,$$
$$M_B = A_B\ m_{B\perp}\ \sinh(y^B) = -(M_A + M_C)$$

$$E_{tot} = 2 A_{Pb}\, m_N\ \cosh(y_0)$$

$$E_A = A_P\, m_N\ \cosh(y_0),$$
$$E_C = A_T\, m_N\ \cosh(-y_0),$$

give the spectator numbers, A_P and A_T,

$$M_A = A_P\, m_N\ \sinh(y_0),$$
$$M_C = A_T\, m_N\ \sinh(-y_0),$$

$$y_E^{CM} \approx y^B = \mathrm{artanh}\left(\frac{M_A + M_C}{E_{tot} - E_A - E_C}\right)$$

Making Rotation Visible

The rotation is illustrated by dividing the upper / lower part (blue/red) of the initial state, and following the trajectories of the marker particles.

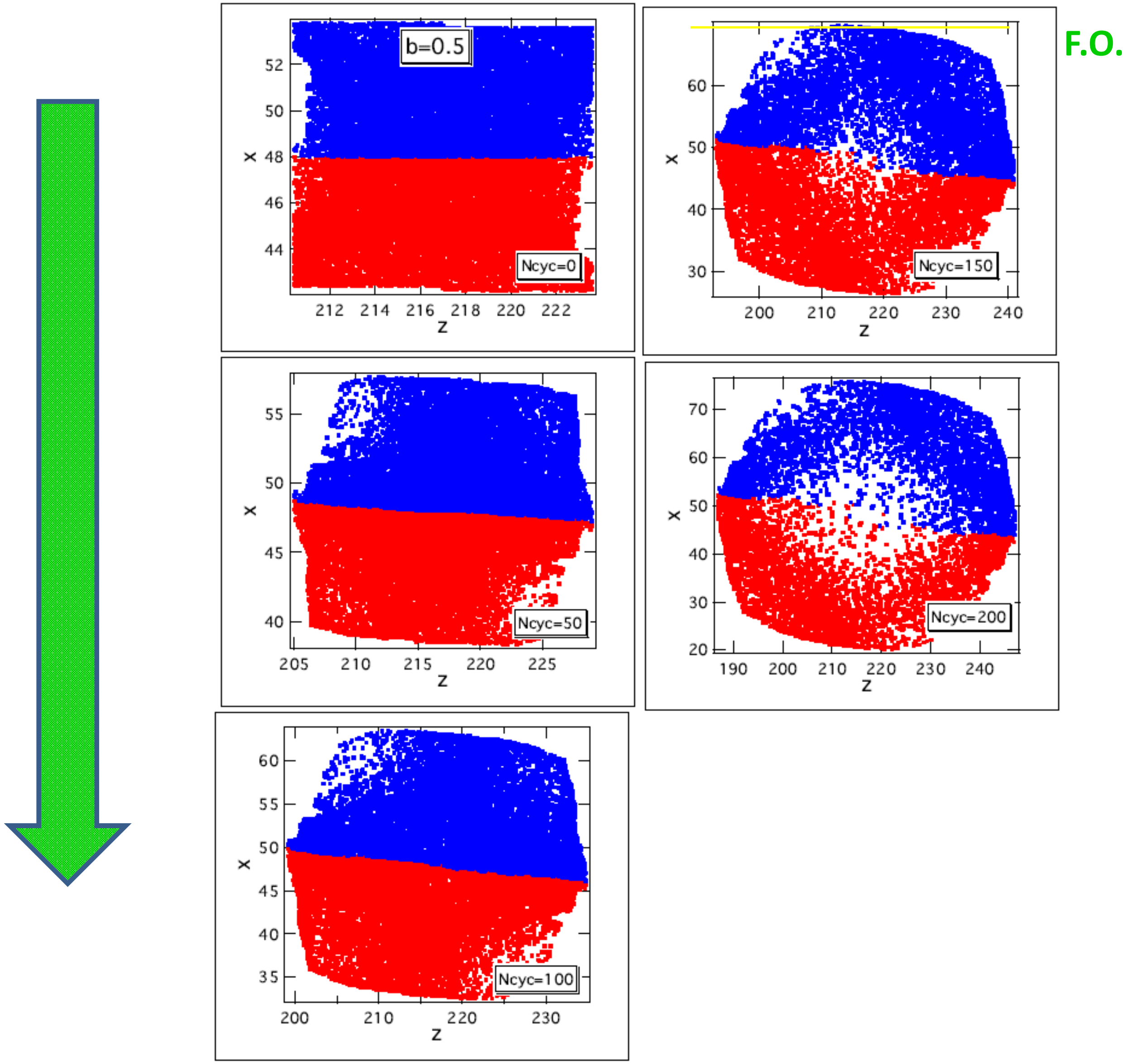

Anti-flow (v1)

FD calculations suggest **measurable v_1(y)** flow at LHC.

These flow parameters are very sensitive to the initial state y_CM-fluctuations, which can and should be measured by ALICE. The most important our prediction is that the v_1 **peak moves to "forward" direction**, in contrast to lower energies.

This is a result of our **tilted initial state with shear**, in which the effective "angular momentum" from the increasing beam momentum **is superseding the expansion** driven by the pressure.

PRL 97, 152303 (2006) PHYSICAL REVIEW LETTERS week ending 13 OCTOBER 2006

Strongly Interacting Low-Viscosity Matter Created in Relativistic Nuclear Collisions

Laszlo P. Csernai,[1,2] Joseph I. Kapusta,[3] and Larry D. McLerran[4]
[1]Section for Theoretical Physics, Department of Physics, University of Bergen, Allegaten 55, 5007 Bergen, Norway
[2]MTA-KFKI, Research Institute of Particle and Nuclear Physics, 1525 Budapest 114, P. O. Box 49, Hungary
[3]School of Physics and Astronomy, University of Minnesota, Minneapolis, Minnesota 55455, USA
[4]Nuclear Theory Group and Riken Brookhaven Center, Brookhaven National Laboratory, Bldg. 510A, Upton, New York 11973, USA

Viscosity vs. T has a <u>minimum at the 1st order phase transition</u>. This might signal the phase transition if viscosity is measured. At lower energies this was done.

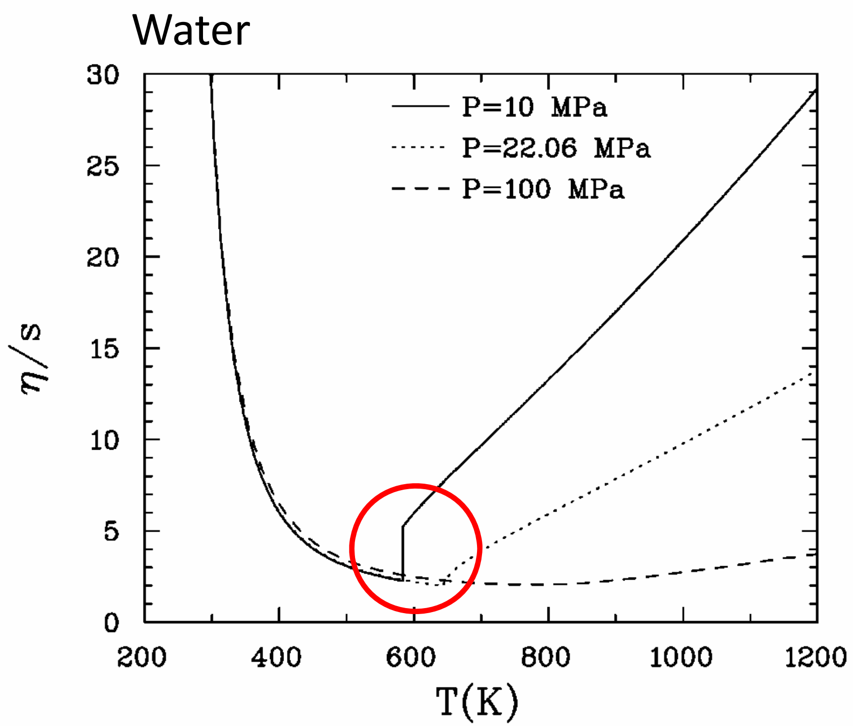

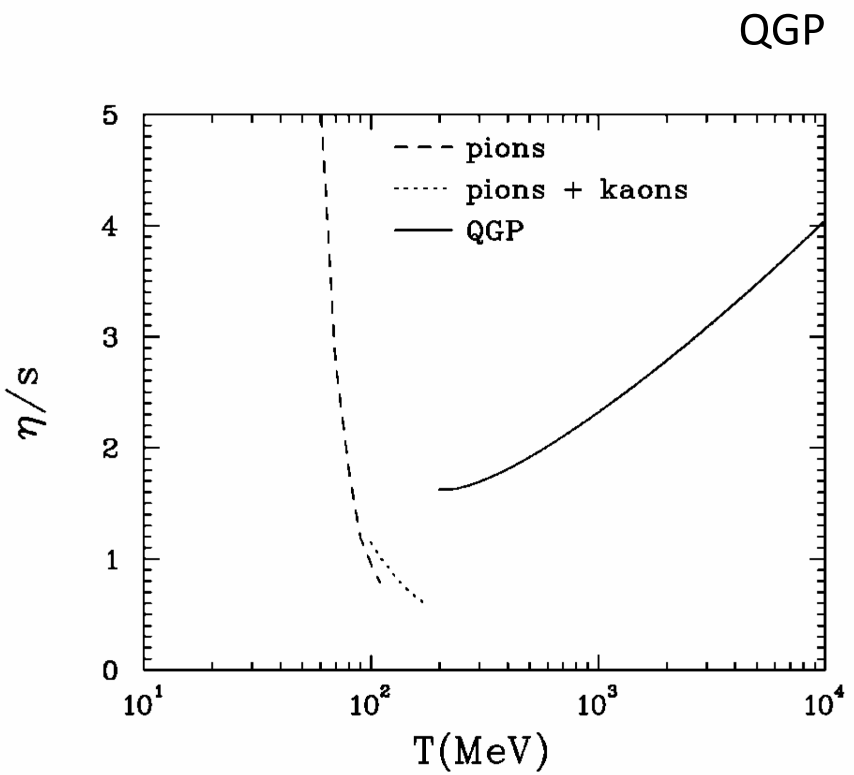

Shear Viscosity – Momentum transfer

[Enskog ~1928]

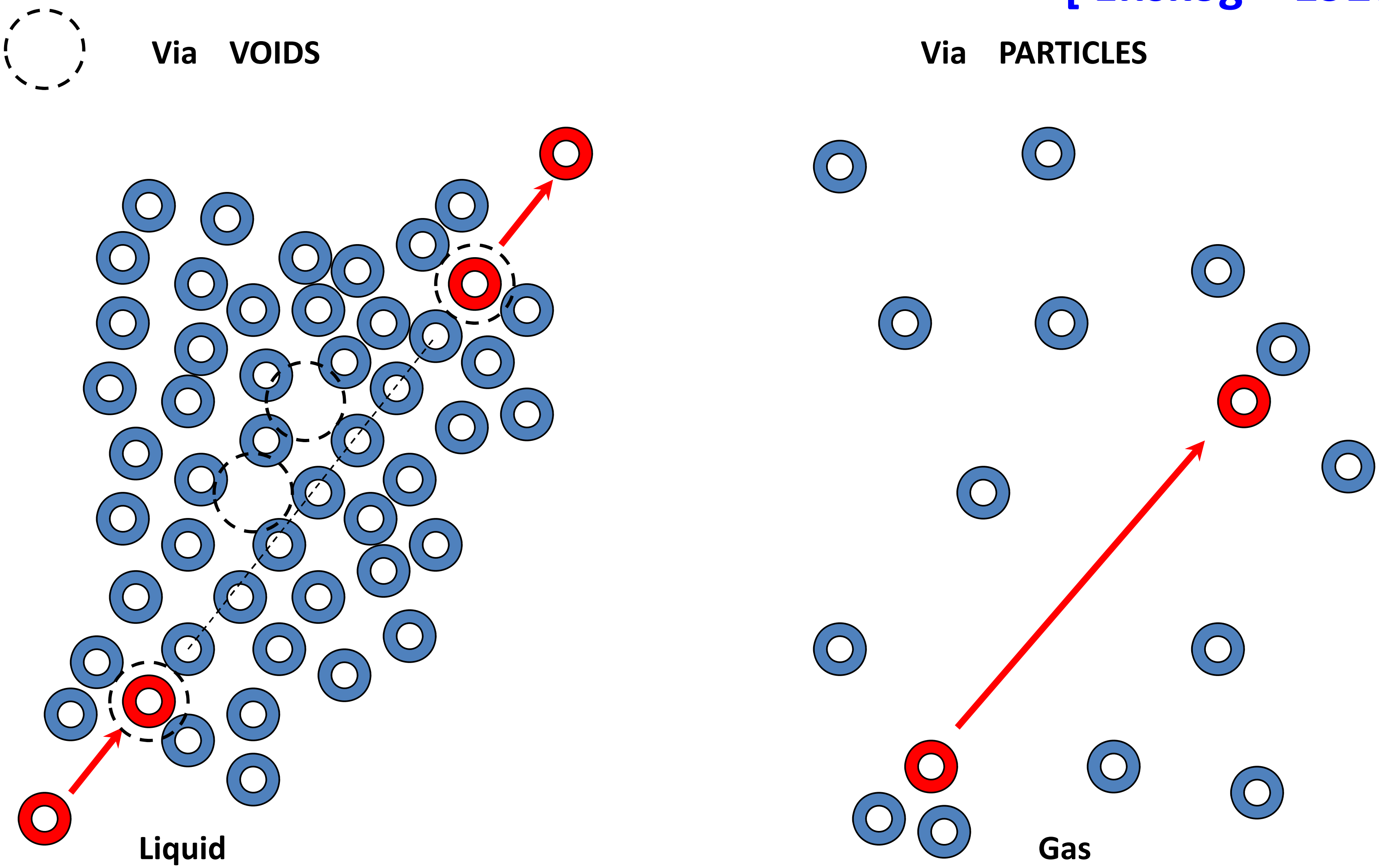

Surfing on breaking waves of Quark-gluon Plasma

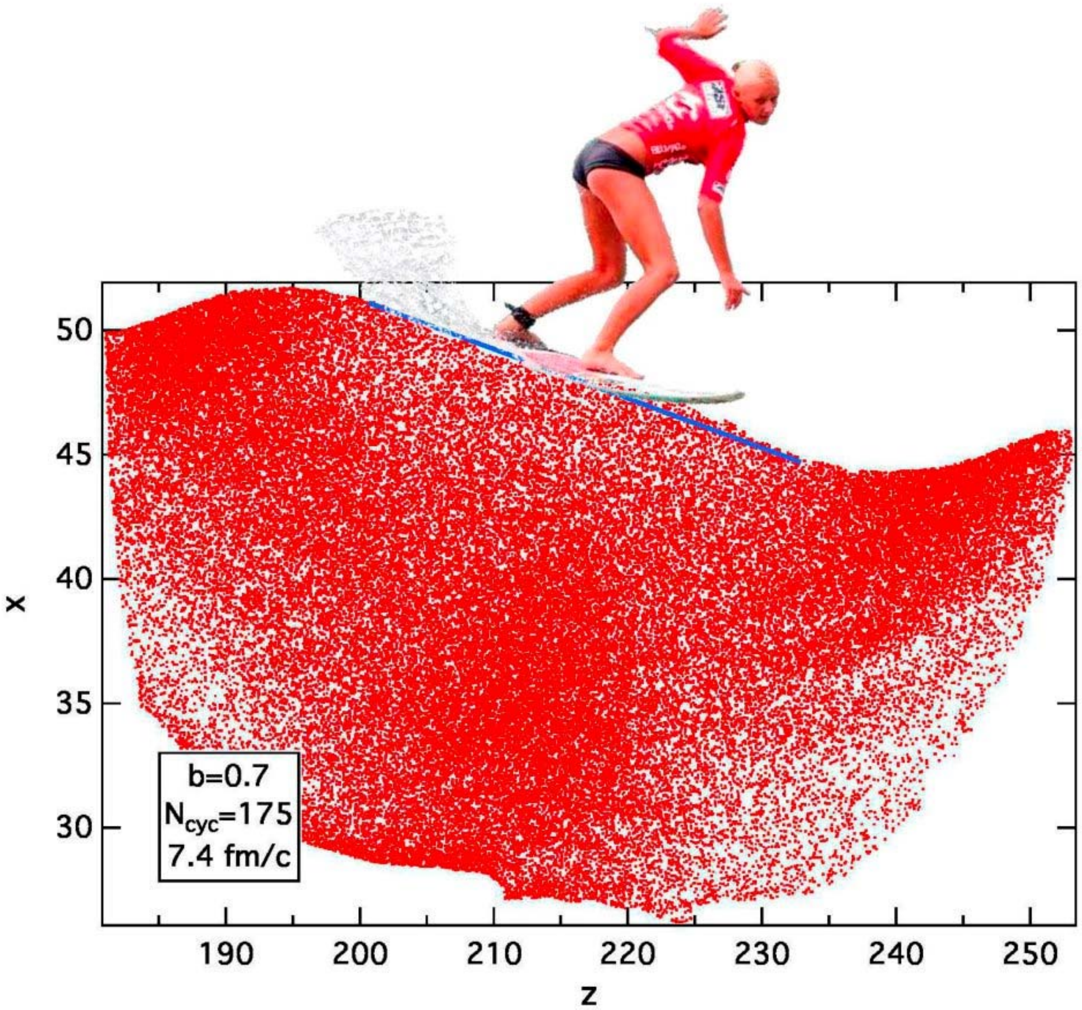

Kelvin-Helmholtz Instability (KHI)

- Turbulent fluctuations are common in **air*** and **water***
- Usually ∃ source*
- Usually damped, but weakly
- ∃ quasi-stationary and developing instabilities
- For KHI the source is shear-flow

The Kelvin – Helmholtz instability

- Initial, almost sinusoidal waves

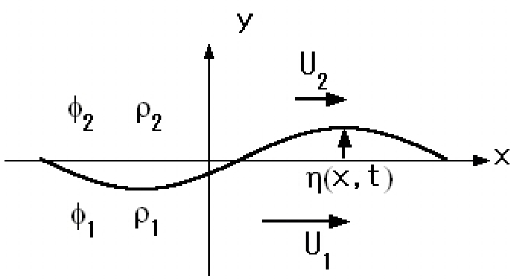

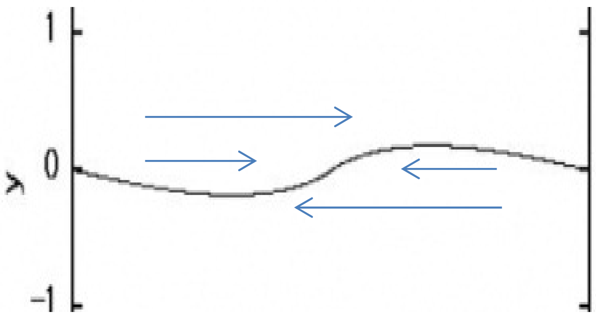

- Well developed, non-linear wave

The interface is a layer with a finite thickness, where viscosity and surface tension affects the interface. Due to these effects singularity formation is prevented in reality. The roll-up of a sheet is observed

[Chihiro Matsuoka, Yong Guo Shi, Scholarpedia]

Kelvin-Helmholtz instability in high-energy heavy-ion collisions

L.P. Csernai[1,2,3], D.D. Strottman[2,3], and Cs. Anderlik[4]

PHYSICAL REVIEW C **85**, 054901 (2012)

arXiv:1112.4287v3 [nucl-th]

KHI →

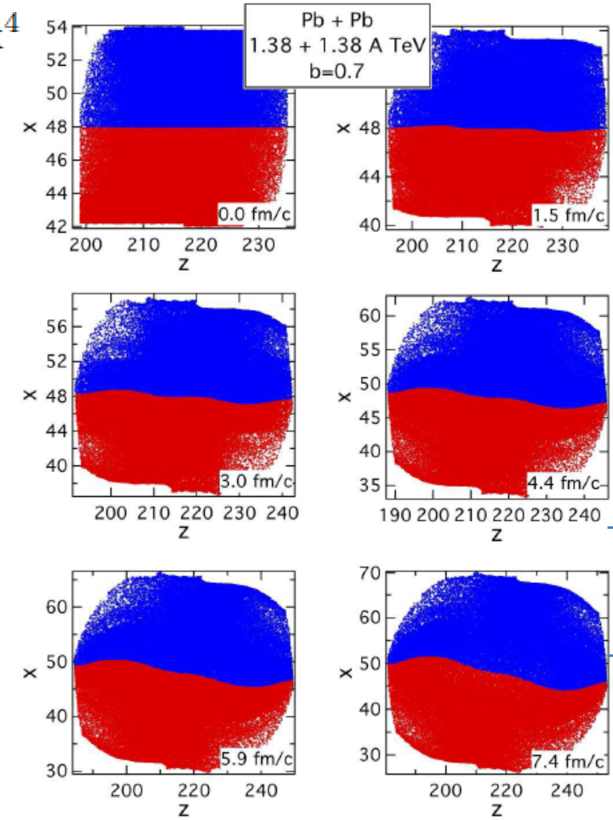

2.4 fm

ROTATION

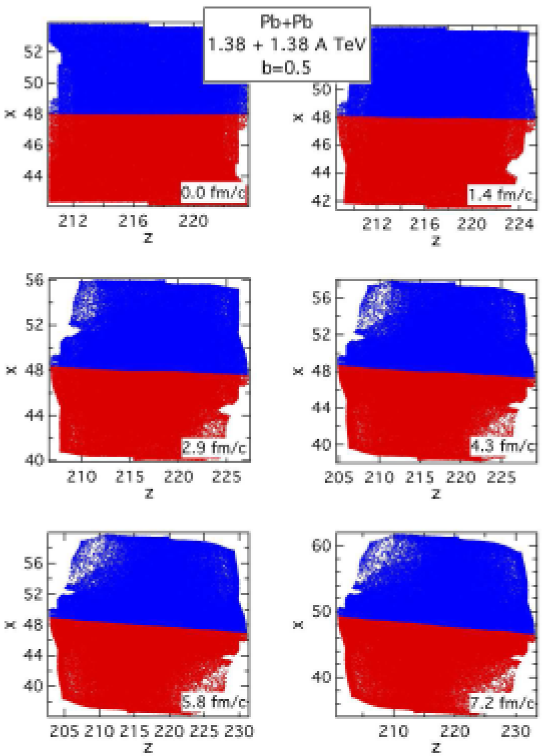

KHI

FIG. 1: (color online) Growth of the initial stage of Kelvin-Helmholtz instability in a $1.38A + 1.38A$ TeV peripheral, $b = 0.7b_{\max}$, Pb+Pb collision in a relativistic CFD simulation using the PIC-method. We see the positions of the marker particles (Lagrangian markers with fixed baryon number content) in the reaction plane. The calculation cells are $dx = dy = dz = 0.4375$fm and the time-step is 0.04233 fm/c The number of randomly placed marker particles in each fluid cell is 8^3. The axis-labels indicate the cell numbers in the x and z (beam) direction. The initial development of a KH type instability is visible from $t = 1.5$ up to $t = 7.41$ fm/c corresponding from 35 to 175 calculation time steps).

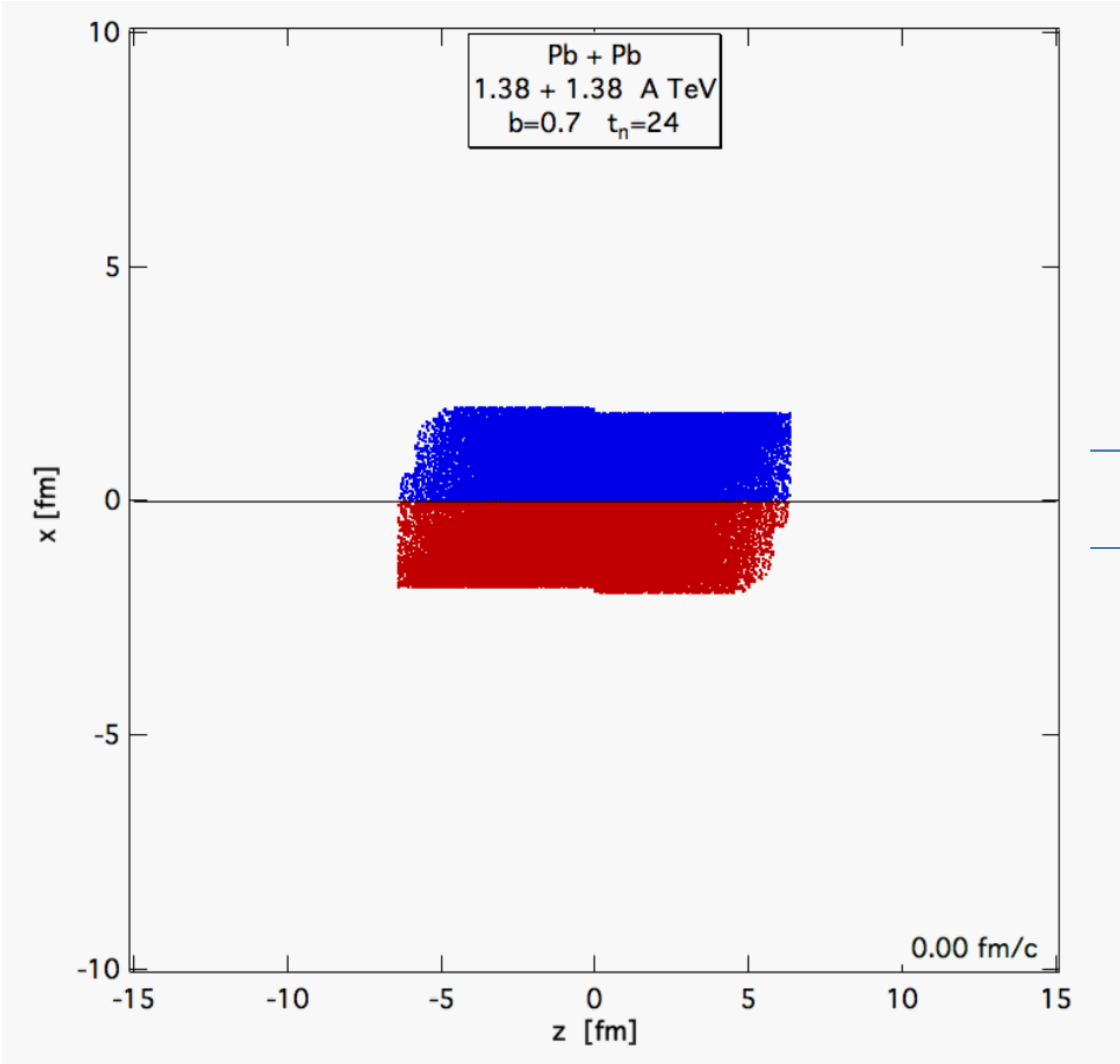
Pb + Pb
1.38 + 1.38 A TeV
b=0.7 t_n=24
0.00 fm/c
x [fm]
z [fm]
10
5
0
-5
-10
-15
-10
-5
0
5
10
15

2.1 fm

The Kelvin – Helmholtz instability (KHI)

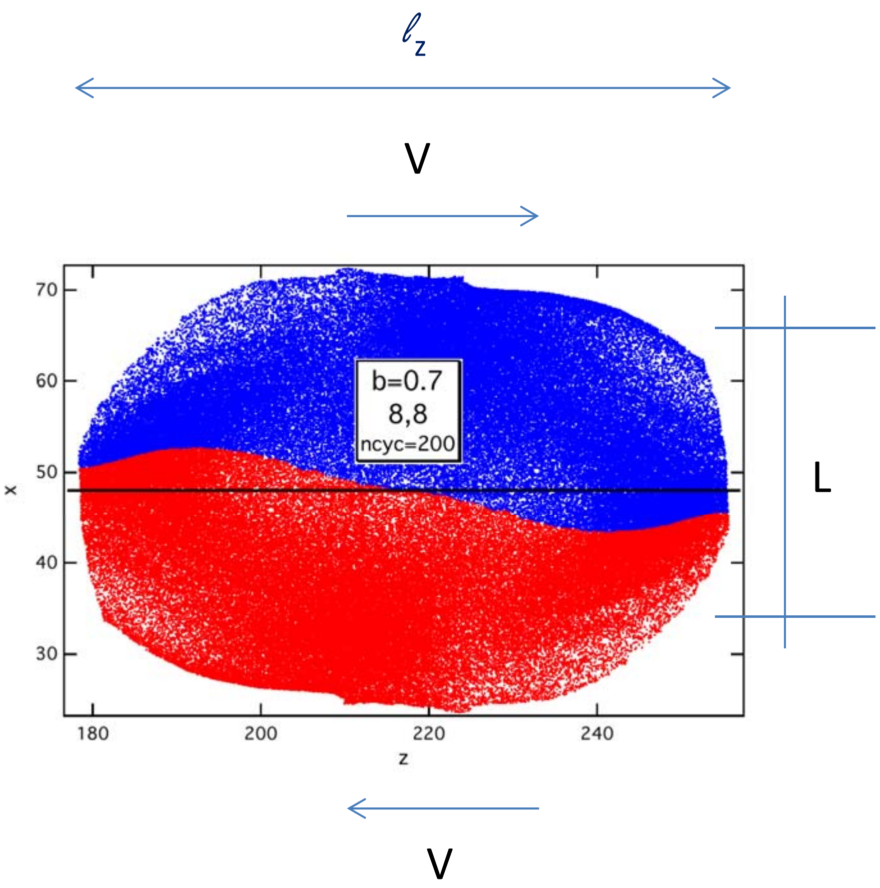

Our resolution is $(0.35 \text{fm})^3$ and 8^3 markers/fluid-cell → ~ 10k cells & 10Mill m.p.-s

- Shear Flow:
- L=(2R-b) ~ 4 – 7 fm, init. profile height
- ℓ_z =10–13 fm, init. length (b=.5-.7b_{max})
- V ~ ±0.4 c upper/lower speed →
- Minimal wave number is k = .6 - .48 fm^{-1}
- KHI grows as $\propto \exp(st)$, where $s = kV$ →
- Largest k or shortest wave-length will grow the fastest.
- The amplitude will double in 2.9 or 3.6 fm/c for (b=.5-.7b_{max}) without expansion, and with favorable viscosity/Reynolds no. Re=LV/ν .
- → this favors large L and large V

The Kelvin – Helmholtz instability (KHI)

- **Formation of critical length KHI (Kolmogorov length scale)**
- ∃ critical minimal wavelength beyond which the KHI is able to grow. Smaller wavelength perturbations tend to decay. (similar to critical bubble size in homogeneous nucleation).
- **Kolmogorov**: $\lambda_{Kol} = [\nu^3/\epsilon]^{1/4}.$
- Here $\epsilon = \dot{e}/\rho \quad \propto \quad T\dot{\sigma}/\rho \quad \propto \quad \nu,$ is the specific dissipated flow energy.
- We estimated: $$\lambda_{Kol} = \begin{cases} 2.1 \div 5.4 \text{ fm for } b = 0.5 b_{max} \\ 1.4 \div 3.6 \text{ fm for } b = 0.7 b_{max} \end{cases}$$
- It is required that $l_z > \lambda_{Kol}$. → we need b > 0.5 b_{max}
- Furthermore
  Re = 0.3 – 1 for "$\eta/s = 1$" and
  Re = 3 – 10 for "$\eta/s = 0.1$"

Very late, post-FO stage: t = 10.16 fm/c

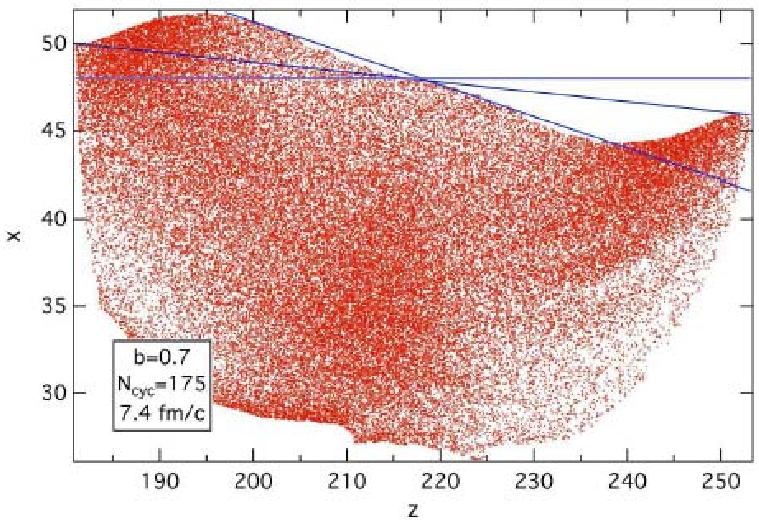

FIG. 5: (color online) The detailed view of the marker particle positions in the lower half of the initial state markers after 175 time-steps. A $1.38A + 1.38A$ TeV energy Pb+Pb peripheral collision is shown, at $b = 0.7\ b_{\max}$ impact parameter with $7^3 = 343$ markers per initial, normal density fluid cell resolution. The lines across the collision center point indicate the initial dividing axis, the change of this axis due to rotation and the additional change of rotation arising from the start-up of a Kelvin-Helmholtz type of instability. This additional effect more than doubles the rotation. In this calculation the cell size is $dx = dy = dz = 0.35$ fm, with a total number of 1814814 marker particles.

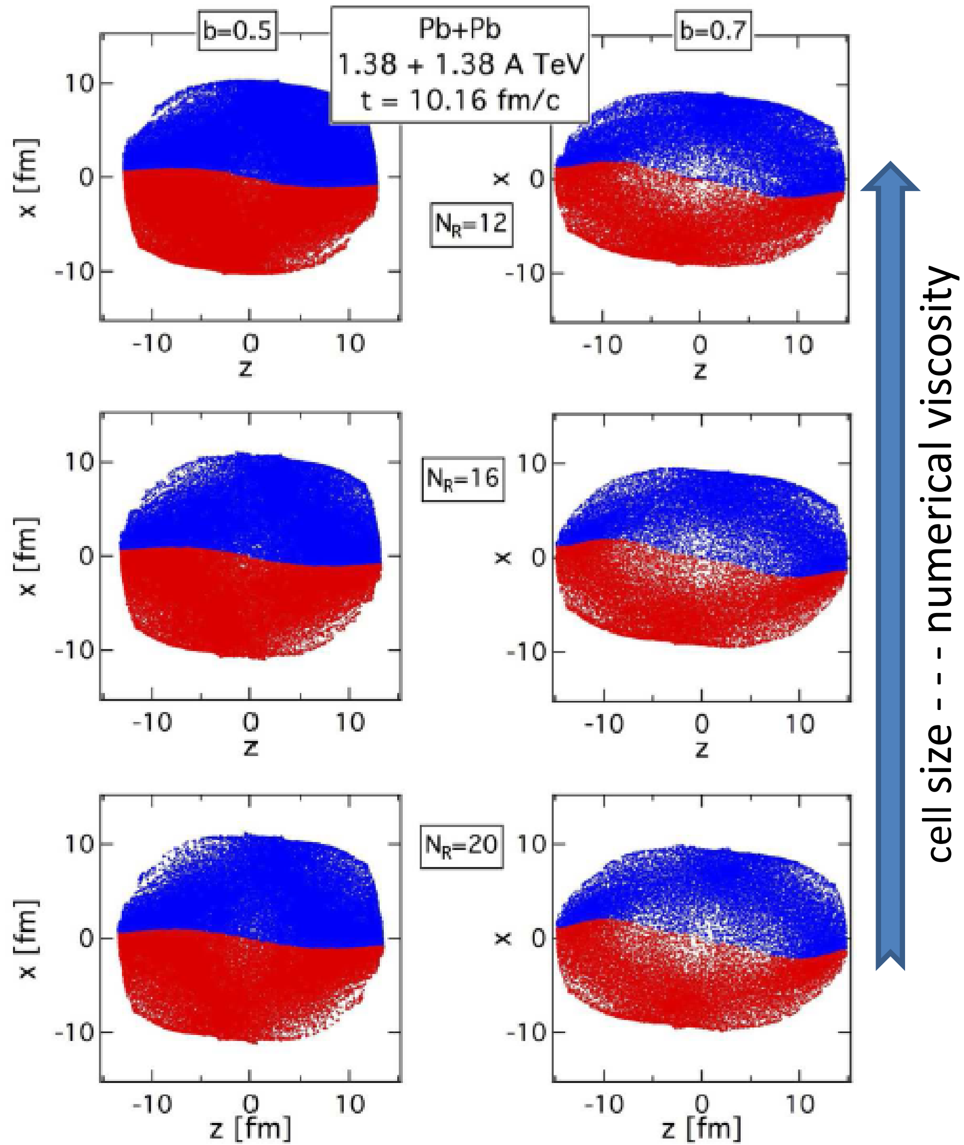

$$\Omega(z,x) \equiv w(z,x)\omega(z,x)$$

$$w_{ik} \equiv (N_{cell}/E_{tot}) \quad E_{ik}.$$

Classical

$$\omega_y \equiv \omega_{xz} \equiv \frac{1}{2}(\partial_z v_x - \partial_x v_z)$$

Relativistic

$$\Theta \equiv \nabla_\mu u^\mu = \partial_\mu u^\mu,$$

$$\omega^\mu_\nu \equiv \frac{1}{2}(\nabla_\nu u^\mu - \nabla^\mu u_\nu),$$

If $\partial_\tau u^\mu \equiv \dot{u}^\mu = u^\alpha \partial_\alpha u^\mu$ is negligible

$$\omega^x_{\ z} = -\omega^z_{\ x} = \frac{1}{2}(\partial_z \gamma v_x - \partial_x \gamma v_z) = \frac{1}{2}\gamma(\partial_z v_x - \partial_x v_z) + \frac{1}{2}(v_x \partial_z \gamma - v_z \partial_x \gamma)$$

$\Omega(z,x)$ $\Omega(z,x)$

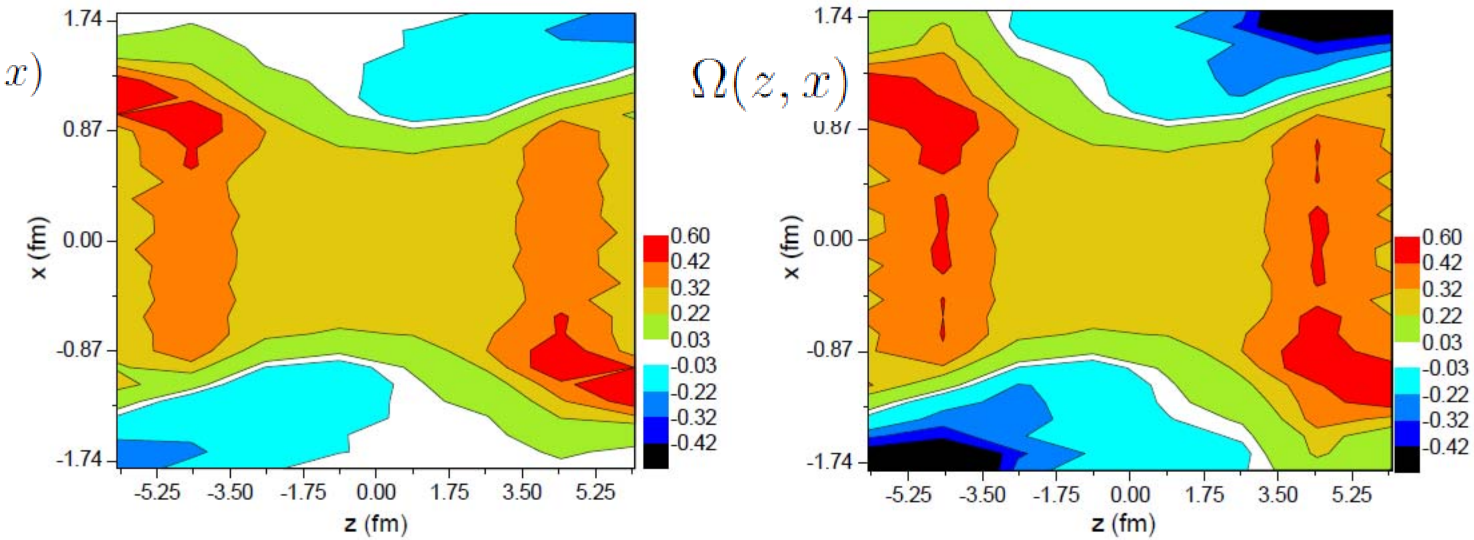

FIG. 1: The classical (left) and relativistic (right) weighted vorticity calculated in the reaction [x-z] plane at t=0.17 fm/c. The collision energy is $\sqrt{s_{NN}} = 2.76$ TeV and $b = 0.7 b_{max}$, the cell size is $dx = dy = dz = 0.4375 fm$.

Relativistic

Classical

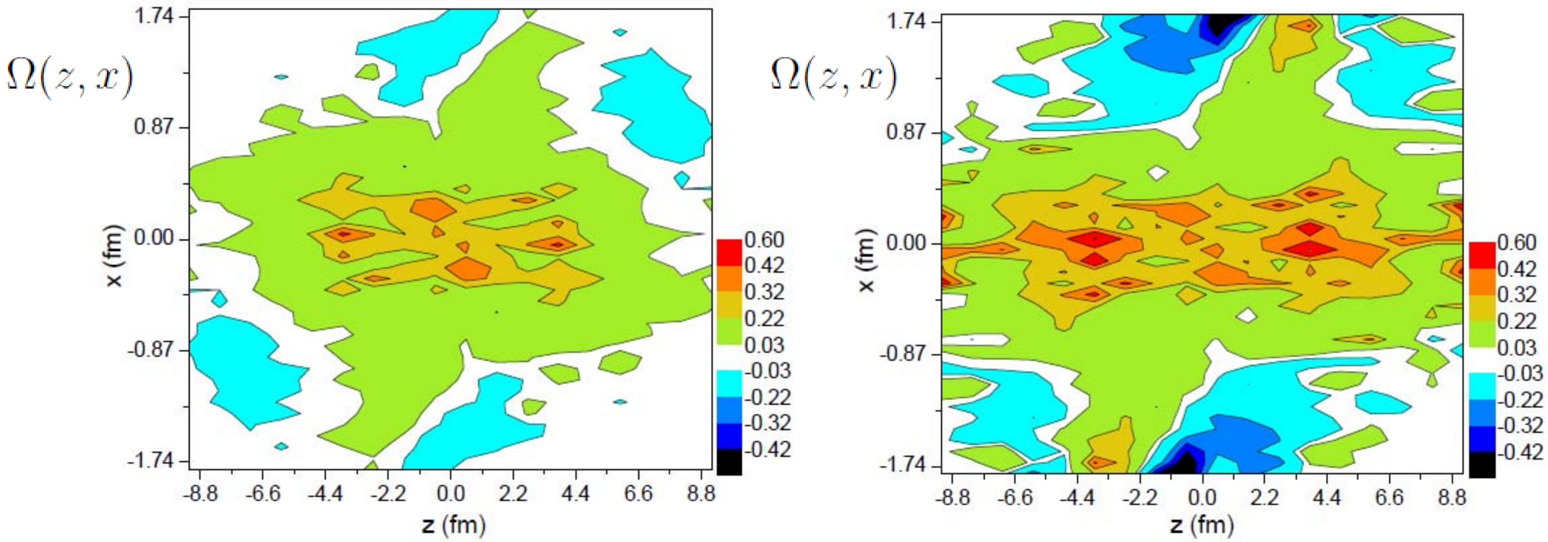

FIG. 2: The classical (left) and relativistic (right) weighted vorticity calculated in thereaction [x-z] plane at $\boxed{t{=}3.56\ \text{fm/c.}}$ The collision energy is $\sqrt{s_{NN}} = 2.76$ TeV and $b = 0.7 b_{max}$, the cell size is $dx = dy = dz = 0.4375 fm$.

Classical

Relativistic

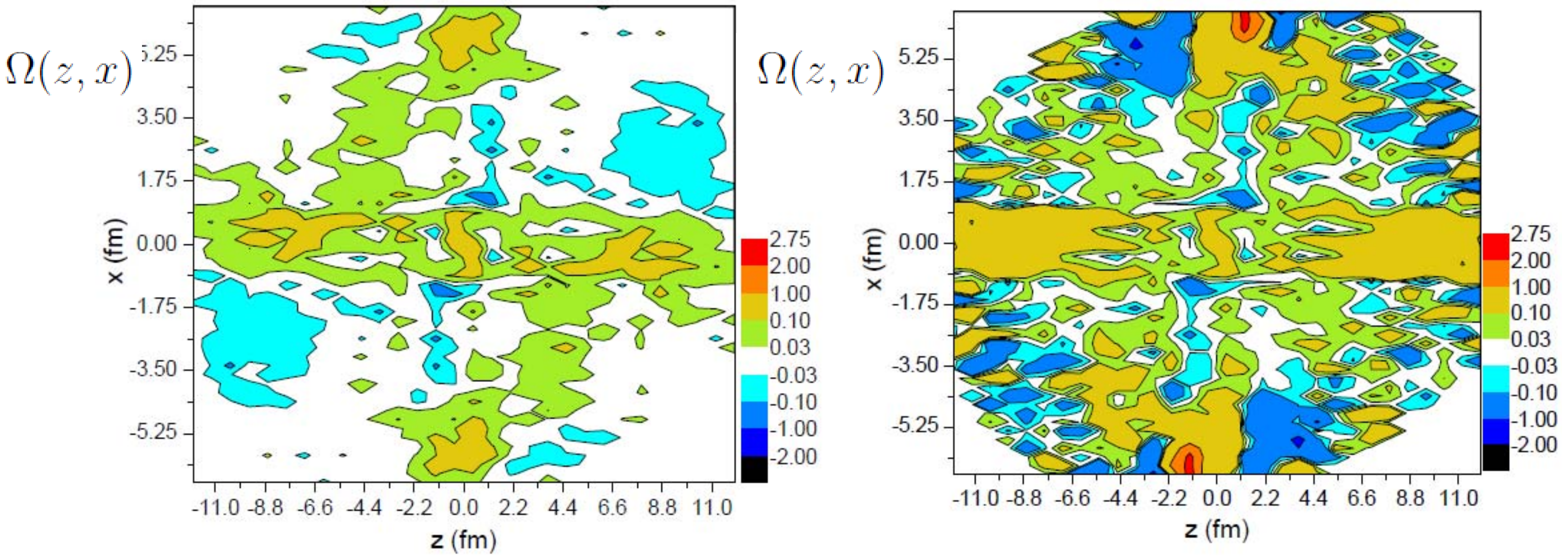

FIG. 3: The classical (left) and relativistic (right) weighted vorticity calculated in thereaction [x-z] plane at $\boxed{\text{t=6.94 fm/c.}}$ The collision energy is $\sqrt{s_{NN}} = 2.76$ TeV and $b = 0.7 b_{max}$, the cell size is $dx = dy = dz = 0.4375 fm$.

Relativistic

Classical

All y-layers

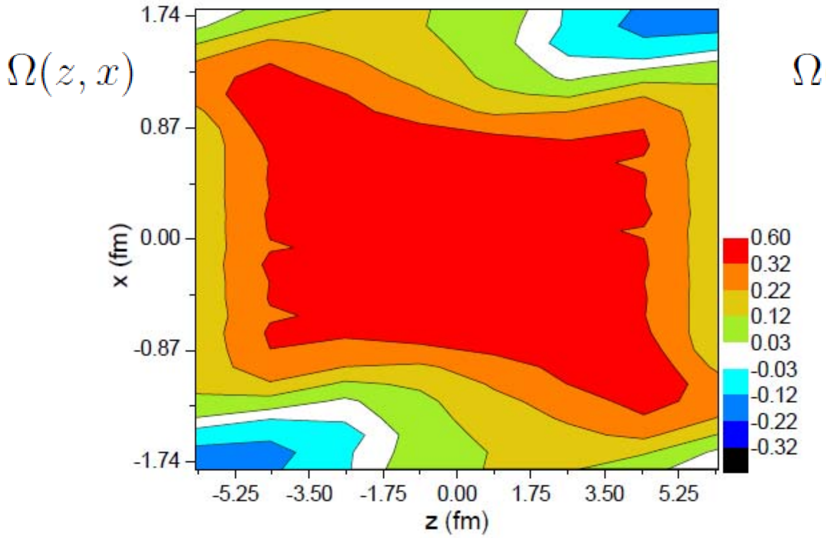

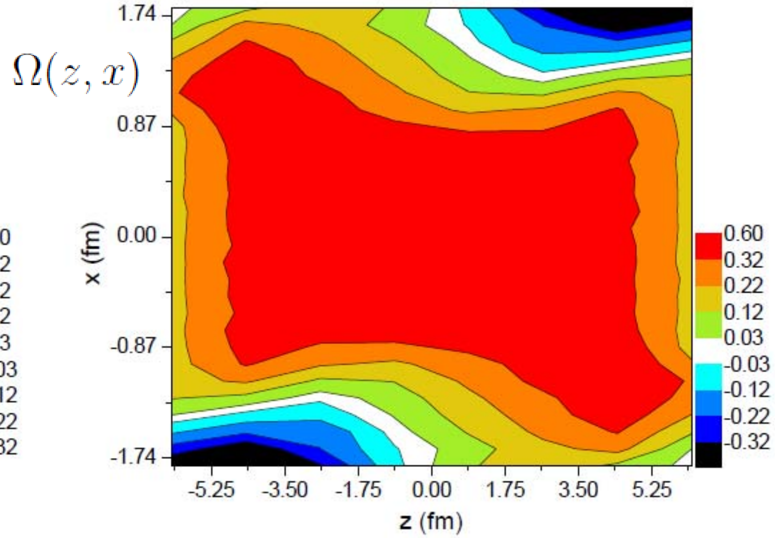

FIG. 4: The classical (left) and relativistic (right) weighted vorticity calculated for all [x-z] layers at $\boxed{\text{t=0.17 fm/c}}$ The collision energy is $\sqrt{s_{NN}} = 2.76$ TeV and $b = 0.7 b_{max}$, the cell size is $dx = dy = dz = 0.4375 fm$.

Relativistic

Classical

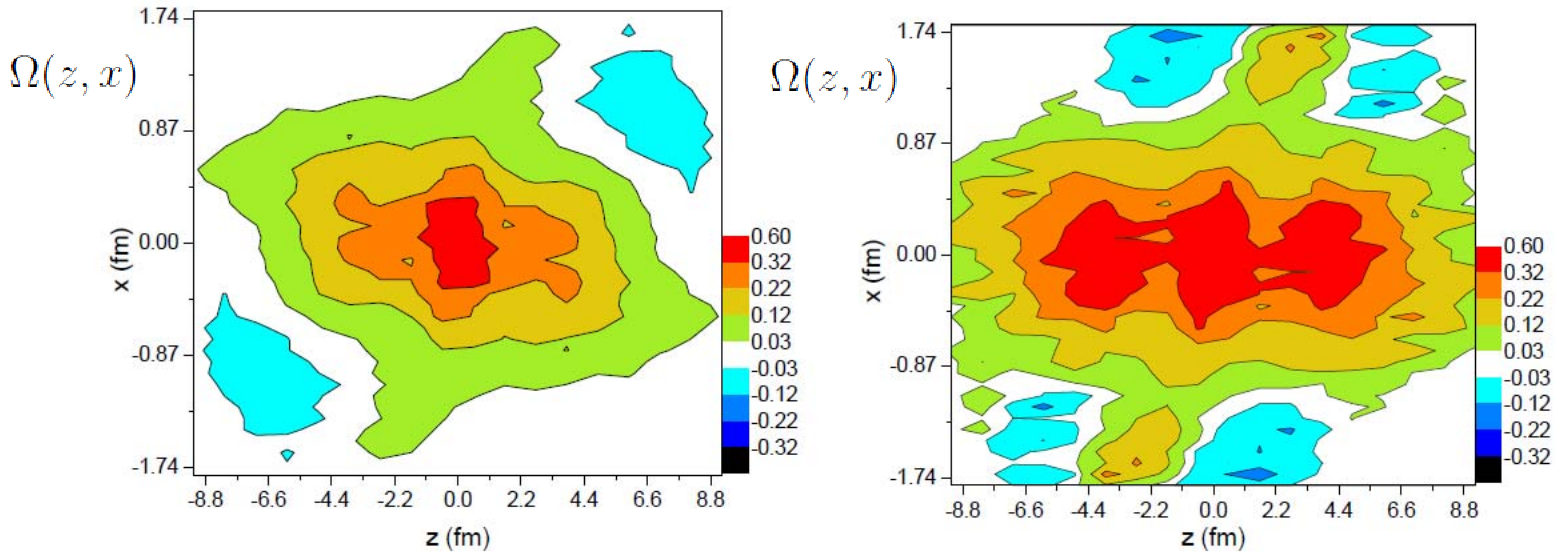

FIG. 5: The classical (left) and relativistic (right) weighted vorticity calculated for all [x-z] layers at t=3.56 fm/c. The collision energy is $\sqrt{s_{NN}} = 2.76$ TeV and $b = 0.7 b_{max}$, the cell size is $dx = dy = dz = 0.4375 fm$.

Relativistic

Classical

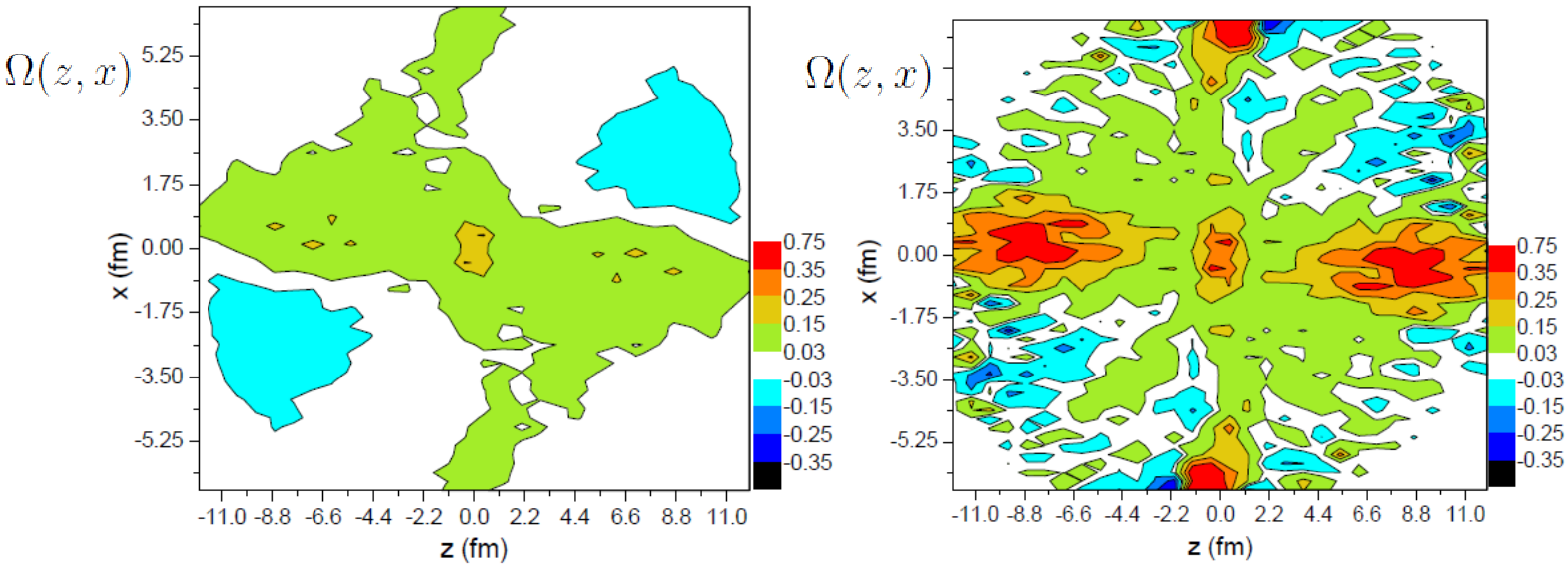

FIG. 6: The classical (left) and relativistic (right) weighted vorticity calculated for all [x-z] layers at t=6.94 fm/c. The collision energy is $\sqrt{s_{NN}} = 2.76$ TeV and $b = 0.7 b_{max}$, the cell size is $dx = dy = dz = 0.4375 fm$.

the surface element $S(t)$. Then we can describe the *circulation* along

$$\Gamma(C(t)) = \oint_{C(t)} \mathbf{v} \cdot d\mathbf{l} = \int\int_{S(t)} \vec{\omega} \cdot \mathbf{n}\, dS$$

where ω is the vorticity

$$\vec{\omega} = \ \mathbf{r}ot\ \mathbf{v}$$

The circulation is conserved for perfect incompressible classical fluids.

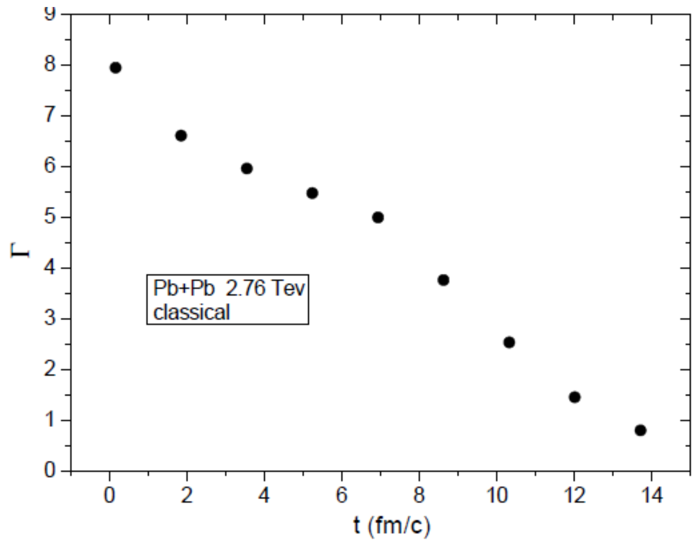

FIG. 7: The time dependence of classical cirulation, $\Gamma(t)$ calculated for all [x-z] layers and then taking the average of the circulations of all layers. The collision energy is $\sqrt{s_{NN}} = 2.76$ TeV and $b = 0.7b_{max}$, the cell size is $dx = dy = dz = 0.4375fm$.

Onset of turbulence around the Bjorken flow

S. Floerchinger & U. A. Wiedemann, JHEP 1111:100, 2011; arXiv: 1108.5535v1

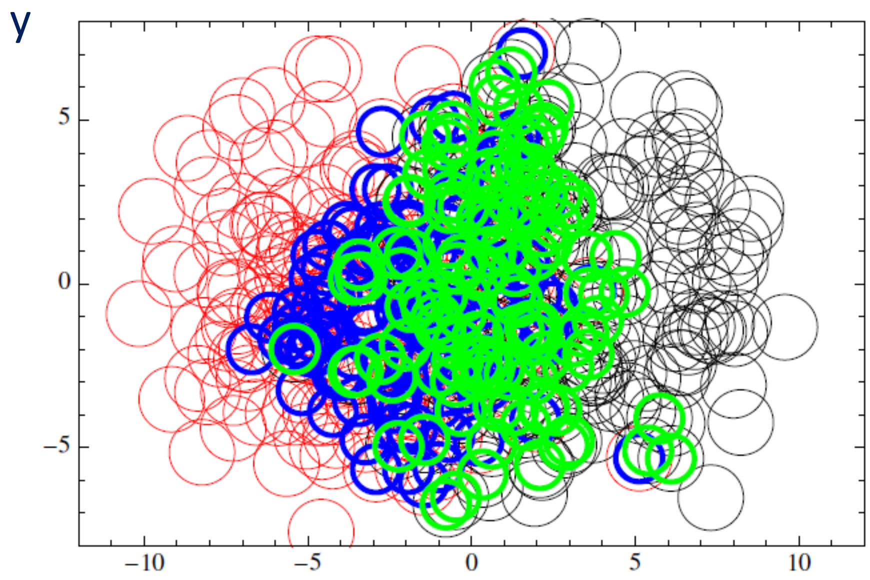

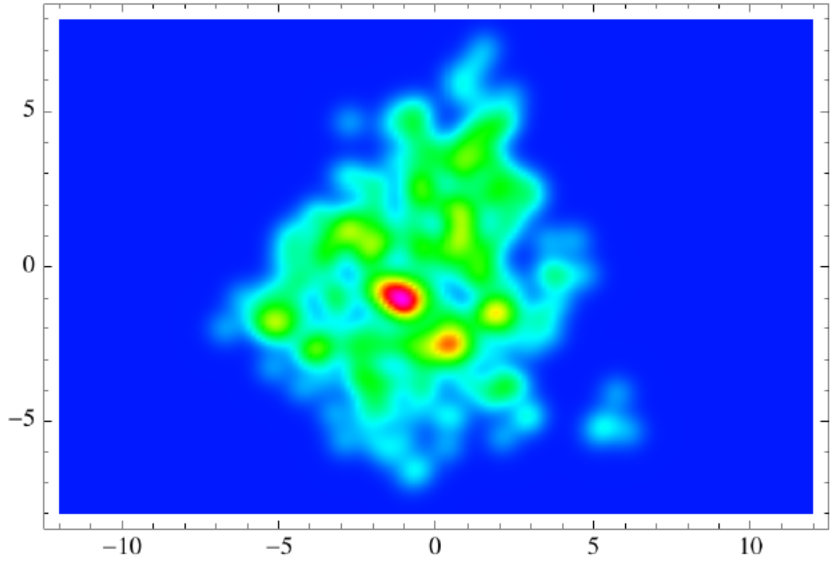

nucleons x [fm] energy density x [fm]

- Transverse plane [x,y] of a Pb+Pb HI collision at $\sqrt{s_{NN}}$=2.76TeV at b=6fm impact parameter
- Longitudinally [z]: **uniform** Bjorken flow, (expansion to infinity), depending on τ only.

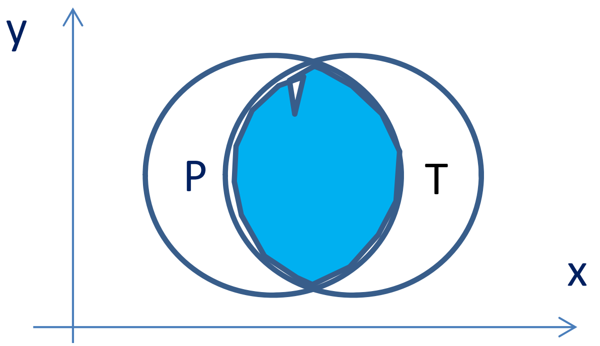

Green and **blue** have the same longitudinal speed (!) in this model. Longitudinal shear flow is omitted.

Onset of turbulence around the Bjorken flow

S. Floerchinger & U. A. Wiedemann, JHEP 1111:100, 2011; arXiv: 1108.5535v1

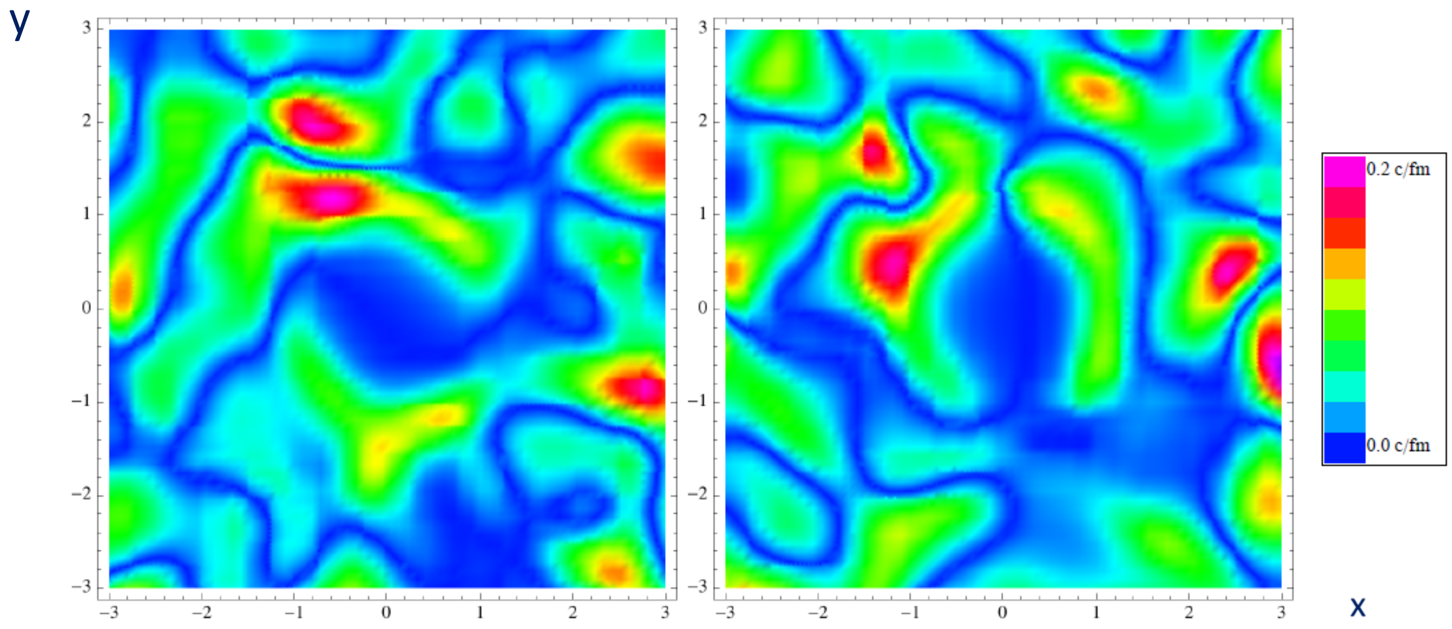

absolute value of vorticity $|\partial_1 u^2 - \partial_2 u^1|$ divergence $|\partial_1 u^1 + \partial_2 u^2|$

- Initial state Event by Event vorticity and divergence fluctuations.
- Amplitude of random vorticity and divergence fluctuations are the same
- In dynamical development viscous corrections are negligible (→ no damping)
- Initial transverse expansion in the middle (±3fm) is neglected (→ no damping)
- High frequency, high wave number fluctuations **may feed** lower wave numbers

Summary

- Flow effects arise from **global** initial asymmetries and **random** initial fluctuations
- These sources can be separated experimentally (at LHC global v_2 & random v_1-v_8)
- New global collective flow effects are predicted, **Rotation** & **KHI**
- These are to be measured yet (*)
- Fluctuations have interesting consequences on the phase transition and hadronization dynamics